Chalcogenide Letters Vol. 12, No. 7, July 2015, p. 389 - 397

MICROSTRUCTURE AND OPTICAL PROPERTIES OF $As_2(S_xSe_{1-x})_3$ GLASSES IN VIS-NIR REGION

N. ZHANG, J. HU, Z. WANG, H. XIAN, S. GU*
State Key Laboratory of Silicate Materials for Architectures, Wuhan University of Technology, Wuhan 430070, China

$As_2(S_xSe_{1-x})_3$ glasses were prepared by the traditional melt-quenching method with As, S and Se of 99.999% purity. We kept the ratio of As/(S+Se) and change the ratio of S/Se in the studied glass series in order to study the influence of the replacement of chalcogen elements on the microstructure and the optical band gap. The compositional evolution of the main Raman scattering frequency of $As_2(S_xSe_{1-x})_3$ bulk glasses was analyzed to investigate the structural changes following the replacement of Se for S. Based on visible-near infrared transmission spectra, We found that the higher temperature or more Se contents shift the optical absorption edge of the glasses to lower photon energies. Compositional dependences of the optical properties are qualitatively analyzed from electronic structural and elementary compositional points of view.

(Received June 12, 2015; Accepted July 31, 2015)

Keywords: Chalcogenide glassses, Structural evolution, Electronic structure, Optical band gap, Raman Scattering

1. Introduction

Chalcogenide glasses are a approved group of glassy materials which always contain one or more of the chalcogen elements of S, Se and Te, bonding with more electropositive elements most commonly As and Ge[1,2]. With better glass-forming ability, low consumption of energy and precious metal of Ge and higher refractive index, As-X(X=S or Se) glasses have been widely studied from 1950s. From the first chalcogenide glass-As_2S_3-to be commercially developed, produced for passive, bulk optical components for mid-IR, attention was focused on the excellent optical properties in mid-IR region[3-5]. The applications of infrared optics, like energy management, thermal fault detection, electronic circuit detection, temperature monitoring, night vision and so on, gained considerable achievements[6]. However, less attention has focused on optical properties in Vis-NIR region. The evolvement rules are not particularly clear. So we tried to extend this work.

The data of Visible-Near Infrared transmission spectra reflect the the absorption coefficient and the band gap directly[7]. Benefiting from the study of XPS valance band spectra and the theoretical basis of Ab initio and other effective methods in recent years, we can get some

* Corresponding author: gsx@whut.edu.cn

useful information about the electronic structure by combining with the transmission spectra and Raman Scattering spectra. Numerous techniques have been used to investigate short- and medium-range orders in $As_2(S_xSe_{1-x})_3$ because it has become apparent that Raman spectroscopy is a simple, direct, and powerful probe of the molecular structure of chalcogenide glasses [8-10]. we hold constant number of the topological constraints in the studied glass series of $As_2(S_xSe_{1-x})_3$, and then change the ratio of the chalcogenide component in order to explore the change of the property.

In this paper, S/Se-rich $As_2(S_xSe_{1-x})_3$ bulk glasses were prepared by the conventional melt-quenching method. E_g^{opt} of different chalcogenide contents and different temperatures ware derived from the visible-near infrared transmission spectra. Through the investigation of Raman spectra, the microstructure of these glasses was analyzed and the origin of compositional evolution of the optical properties of $As_2(S_xSe_{1-x})_3$ glasses in Vis-NIR region was discussed by electronic structural and elementary compositional points of view.

2. Experimental details

Different compositions of bulk $As_2(S_xSe_{1-x})_3$ chalcogenide glasses with x = 0, 0.25, 0.5, 0.75 and 1, where x is the atomic ratio S/(S+Se), were prepared from high purity (99.999%) raw materials by the melt-quenching technique. The raw materials were sealed in evacuated (10^{-2} Pa) quartz ampoules. The rocking furnace was regularly shaken to ensure homogeneousness of the melt. The sealed quartz ampoules were heated for 24 hrs at the temperature range from 1073 K and then maintained at 823 K for 5 hrs without shaking before quenched into ice-cooled water to avoid crystallization. For the details, see the reference. The chalcogenide glass bulks were annealed in order to relieve residual stress and then cut and polished into discs with 1 mm thickness.

Raman spectra were recorded using back-scattering configuration with the resolution of 4 cm^{-1} in the wave number range between 100 and 800 cm^{-1}. The spectra were collected with an Intelligent Fourier infrared spectrometer (Therno Nicolet, Nexus). The 1064 nm laser was used as the excitation light.

Visible-Near Infrared transmission spectra of the samples was recorded within the wavelength range of 300-2600 nm by using a conventional spectrophotometer (Shimadzu, UV-1601).

3. Results and discussion

From the Raman spectra in Fig.1(a), we can see some basic information about the structure of $As_2(S_xSe_{1-x})_3$ glasses. Two main regions located at 200-280 and 280-400cm^{-1} of stretching vibrational mode related to As-Se and As-S, respectively[11, 12]. The Raman spectrum of As_2S_3 has strong peaks in the area at 292, 310, 355 and 382 cm^{-1}. The two shoulders around 312 and 380 cm^{-1} of As_2S_3 Raman spectra are due to interactions among the AsS_3 pyramids. The peak of 340 cm^{-1} in As_2S_3 is attributed to the ν1 mode of AsS_3 pyramid. Meanwhile, two obvious shoulders located at 230 and 248 cm^{-1} in Raman spectra of As_2Se_3 can be attributed to the symmetrical and asymmetrical vibrational modes of $AsSe_3$ pyramid[13]. What's more, in the As-Se

related peak range of $As_2(S_xSe_{1-x})_3$ glasses, the main Raman bands are attributed to the As-Se vibration of [AsS_2Se], [$AsSSe_2$] and [$AsSe_3$] pyramids (230, 241, 257 cm^{-1}) with the vibrational mode of $\nu_1(A')$, $\nu_2(A')$ and $\nu_1(A_1)$, respectively[14,15]. The weak inter-molecular coupling in the As_2S_3 and As_2Se_3 glass systems indicates that the Raman vibrational modes related to interactions among As_2S_3 (As_2Se_3) are much weaker than those related to intra-As_2S_3 (As_2Se_3) pyramids[16].

The normalized broad peaks located at 280-400 and 200-280 cm^{-1} which are related to the main vibrational modes of AsS_3 and $AsSe_3$ pyramids were showed in Fig.1(b) and Fig.1(c) respectively. The relative intensity of the two bands changes monotonically with the substitution of Se for S. With the S contents increases, the peaks in the region 200–280 cm^{-1} moves toward lower frequencies. The small shoulders at 210 and 275 cm^{-1} become weaker and finally disappear with decreasing Se. These can be attributed to the vibrational coupling theory[17]. Coupling of vibrating mode of intra- or inter- groups will lead to the shift of related Raman frequency of molecular clusters toward lower wavenumber. Considering the coupling of inter-groups, the stepwise decrease of environmental As_2Se_3 pyramids around the central As_2Se_3 group having both the same symmetry and approximately equal energy to the central As_2Se_3 group. The substitution of Se by S lead to a decline of vibrational coupling of intra-central $AsSe_3$ pyramid, resulting in a decrease of v1 mode of central $AsSe_3$ pyramid.

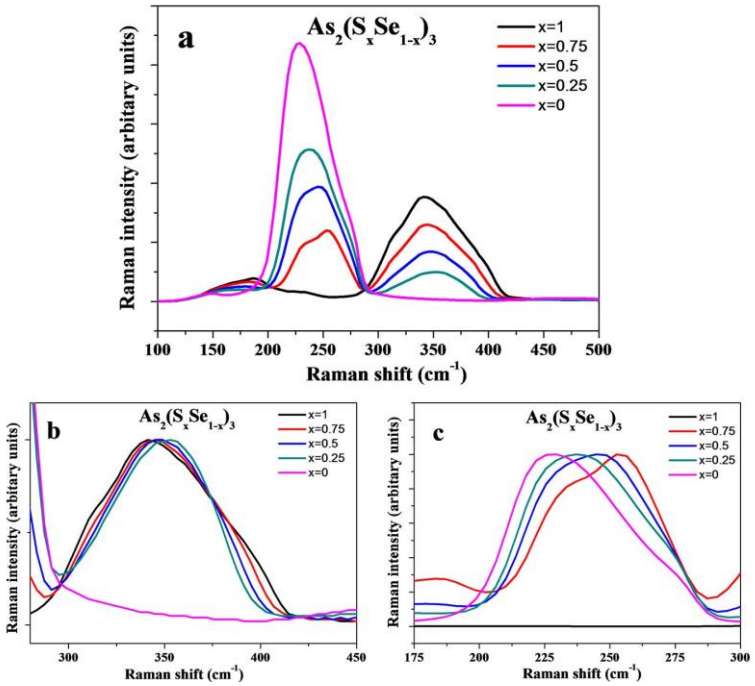

Fig.1 The experimental Raman spectra of the $As_2(S_xSe_{1-x})_3$ glassy system, x=0, 0.25, 0.5, 0.75, 1, b is obtained by normalization processing of peaks positing near 355 cm^{-1}, c is obtained by normalization processing of peaks positing near 248 cm^{-1}

The peak shift in the 280–400 cm^{-1} is less observable, it moves toward higher frequencies with the S contents increases. But the two shoulders at 312 and 380 cm^{-1} also reduce in intensity and finally disappeared with decreasing S. These can be attributed to the electronic induction effect[18]. For AsS_3 group, S-As-S exists generally. With the replacement of Se for S, S-As-Se

formed, which coursed the enhancements of the electronegativity of S atom and the vibrational force constant of As-S. Then the frequency of central AsS_3 pyramids has a gradual increase.

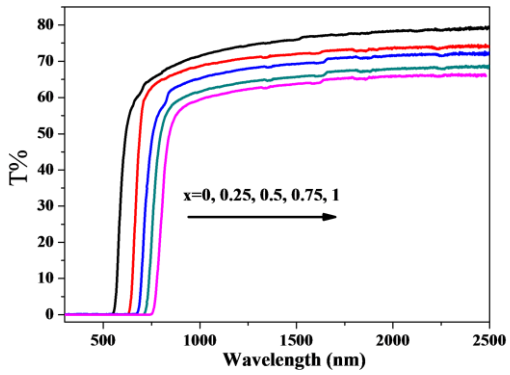

Fig.2 Visible-near infrared transmission spectra of $As_2(S_xSe_{1-x})_3$ glasses

Visible-Near Infrared transmission spectra of $As_2(S_xSe_{1-x})_3$ glasses is showed in Fig.2, light transmitted through the glass sample in infrared bands, but hardly in ultraviolet-visible bands. Like other infrared transparent material, the values of the transmittance of $As_2(S_xSe_{1-x})_3$ glasses are around 70% when the wavelength is higher than 1000 nm. It shows that $As_2(S_xSe_{1-x})_3$ glasses have excellent infrared transmission. With wavelength increases, the transmittance increase. With Se content decrease, the transmittance decrease and short-wave absorption edges have blue shift.

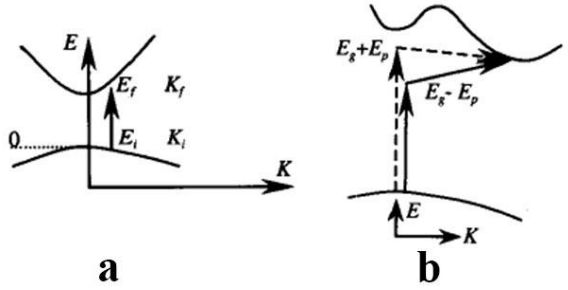

*Fig.3 The sketches of direct interband transition in direct-gap semiconductor(**a,** the relationship of wave vector: $K_i=K_f=K$)*[19] *and indirect interband transition with phonons(b, the relationship of wave vector: $K_i+q=K_f$)*[20]

The absorption coefficient α was calculated by Lambert-Beer's Law[21]

$$\alpha = -\lg T = kcd \tag{1}$$

Where T is the transmission coefficient, k is absorption coefficient, c is the concentration and d is the thickness of the sample. From Lambert-Beer's Law, we get the relationship between photon energy and α of As_2S_3 glasses at different temperatures, which are showed in Fig.4. A stepwise decrease of E_g appeared obviously. We can find some evidence from Fig.4. In the case of a, an electron directly jumps from the valance band to the conduction band with the same wave

vector after absorbing a photon' worth of energy. In the case of b, the maxium of valance band has the different K value from the minimum conduction band. The optical transition from the top of the valance band to the bottom of the couduction band cannot be achieved directly by light irradiation, which is because the wave vector of photo is much smaller than that of electron. So phonon is needed to take part in the interband transition. Absorption coefficient is closely related to lattice temperature when phonon take part in the interband transition, but hardly related to lattice temperature when the electron directly jumps from the valance band to the conduction band without phonon[22]. From Fig.4, absorption edges have shift obviously. Therefore, we judge, $As_2(S_xSe_{1-x})_3$ glasses are indirect interband transition amorphous substance.

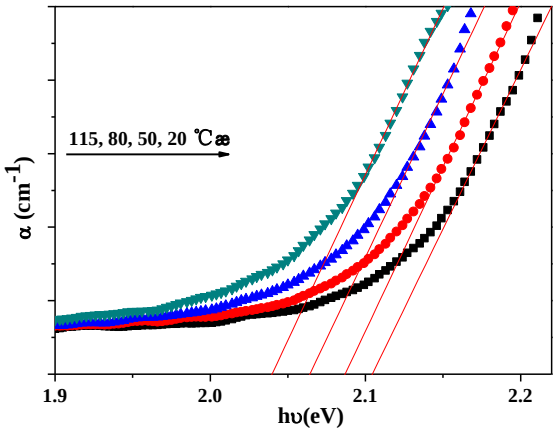

Fig.4 The relationship between α and photon energy of As_2S_3 glasses at different temperatures

In the strong absorption region of the absorption spectra (the absorption coefficient $\alpha>10^4$ cm^{-1}), according to the model proposed by Tauc[22], the absorption coefficient is given by the following quadratic equation

$$\alpha h\nu = B(h\nu - E_g^{opt})^m$$

Where h is Planck's constant, ν is the frequency, B is the Tauc parameter and E_g^{opt} is the optical energy gap in the investigated glasses. m is the coefficient depends on the mode of electron transition. For amorphous materials, m=1/2 corresponding to direct allowed interband transition and m=2 corresponding to indirect allowed interband transition. We can derive the value of E_g^{opt} for indirect allowed interband transition from $\alpha=0$ intersects of $(\alpha h\nu)^{1/2}$ in Fig.5.

For indirect allowed interband transition, E_g^{opt} of $As_2(S_xSe_{1-x})_3$ (x=0, 0.25, 0.5, 0.75, 1) are about 1.50 eV, 1.58 eV, 1.67 eV, 1.79 eV and 2.01 eV respectively. The well fitted curves indicate that indirect allowed interband transition model should be the mechanism responsible for the optical absorption in this spectral region of the $As_2(S_xSe_{1-x})_3$ bulk glasses.

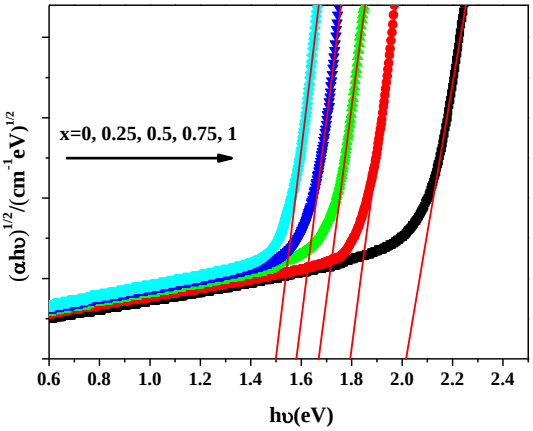

Fig.5 The relationship between (ah ν)$^{1/2}$ and photon energy of $As_2(S_xSe_{1-x})_3$ glasses

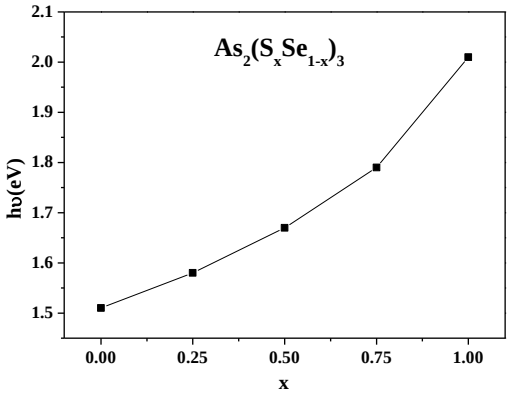

Fig.6 The relationship between the content of S and E_g^{opt}

From *Fig.4* and *Fig.6*, the difference of AsS_3 and $As_2(S_{0.75}Se_{0.25})_3$ is more larger than any other difference. What's more, a stepwise decrease trend of the difference with a increasing Se. The electron density of chalcogenide glasses consist of the valence band formed by bonding(σ) orbitals and the conduction band formed by anti-bonding(σ*) orbitals[23]. From XPS valance band of As-S or As-Se, the structure of the valance band of As-S-Se can be gained by analyzing. Lone pair electrons of chalcogen atoms, which are contributed by every chaslcogen atom, are taking up the top of the valance band. As 4p bonding states give a peak contributed by As-S/As-Se near the VBM in XPS VB[24]. Se 4p or S 3p bonding states associated with Se-Se and S-S covalent bonds below As 4p bonding states. Chalcogenide atoms are known to form the basis of the valence band by lone-pair electron states. The lone pair electrons interact with the π-orbitals. Lone pair electrons of chalcogen atoms play dominant role in the formation of valence band electronic structure of chalcogen glasses. By the calculation of the electronic DOS for As-Chalcogen, the bottom of the conduction band is composed of the anti-bonding states of S 3p/Se 4p and As 4s orbitals.[25, 26]. Based on the above analysis, Scheme of the energy band-structure near the band gap of As-S-Se was given in Fig.7.

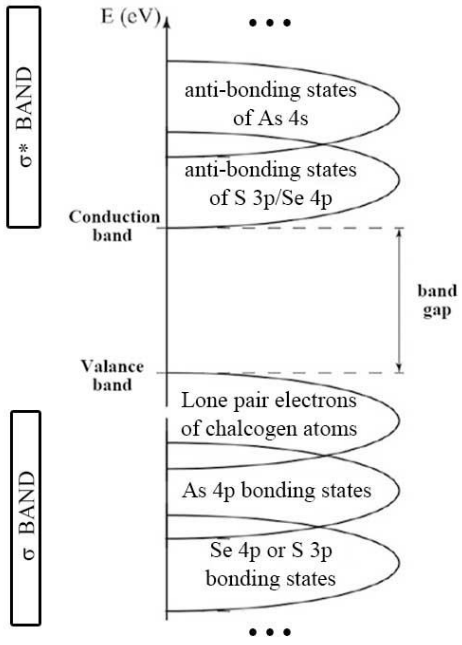

Fig.7 The energy band-structure scheme near the band gap of As-S-Se

For As_2S_3 glass, with the replacement of Se for S, VBM transferred from lp S to lp Se rapidly. It can be concluded in macroscopical phenomenon that the absorption edges have a big shift to lower wavelength and E_g^{opt} diminish greatly. When remain the replacement of Se for S continuously, more lp electrons of Se atoms go into the VBM, which widen the energy band and increasing the electronic density. So the the tendency of change of absorption edges became smaller. We should note here is that the main contribution of this process is improving the condition for electron transition at the original position of lp Se electron, not at a new position of VBM.

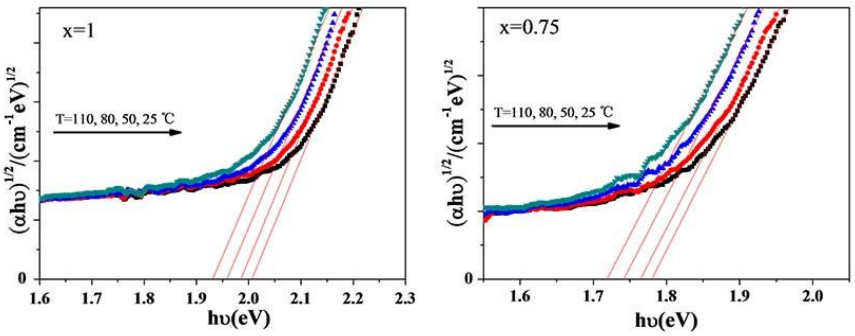

Fig.8 The relationship between $(ah\nu)^{1/2}$ and photon energy of $As_2(S_xSe_{1-x})_3$ glasses at different temperatures

The temperature dependence between $(\alpha h\nu)^{1/2}$ and photon energy of As-S-Se glasses are showed in Fig.8. With the elevation of temperature, the curves shift to lower photon energy. At the

linearity region of low absorption coefficient, the slope of absorption edge depended on phonon absorption[20]. At the linearity region of high absorption coefficient, the slope of absorption edge depended on phonon emission[27]. No matter phonon absorption or phonon emission, the slope increase with the elevation of temperature, which lead to a red shift of absorption edge and a increase of E_g^{opt}.

4. Conclusions

Systematic measurements of compositional evolution of Raman scattering frequency of $As_2(S_xSe_{1-x})_3$ glassy samples have been conducted. Based on the proposed electronic structural model and short-range order, the shift of transmission spectra and the mutative values of E_g^{opt} based on contents or temperatures can be reasonably explained and the spectral evolutions can be successfully elucidated. At the same time, the following conclusions can be deduced:

1. The shift of the main Raman peaks can be attribute to the changed chemical environment: electronic induction effect and vibrational coupling theory.

2. It support by the obvious shift of absorption edge at various temperatures that chalcogenide glass is indirect bandgap semiconductor.

3. With the replacement of Se for S, E_g^{opt} decreases quickly at the first and subsequently the reduction rate of E_g^{opt} slows down, which can be mainly ascribed to the shift of VBM.

4. With the elevation of temperature, the curves of $(\alpha h\nu)^{1/2}$ and photon energy shift to lower photon energy, which can be attribute to the effect of phonon absorption and phonon emission.

Acknowledgments

This work was supported by NSFC (nos. 51372180, 51272072, 51172169), NCET (no.NCET-11-0687) and the key technology innovation project of Hubei Province (Nos.2013AEA005, 2013AAA005).

References

[1] A Zakery, S R Elliott. Journal of Non-Crystalline Solids, **330**, 1 (2003).
[2] AB Seddon. Journal of Non-Crystalline Solids, **184**, 44 (1995).
[3] B Bureau, X Zhang, Smektala F. Journal of non-crystalline solids, **345**, 276 (2004).
[4] SX Gu, DX Pi, HZ Tao, Q Zeng, XJ Zhao, HT Guo, HY Chen. Journal of Non-Crystalline Solids, **383**, 205 (2014).
[5] RK Pan, HZ Tao, JZ Wang, HF Chu, TJ Zhang, DF Wang, XJ Zhao. OPTIK, **124**, 4943 **(**2013).
[6] CG Lin, HZ Tao, XL Zheng, RK Pan, HC Zang, XJ Zhao. Optics Letters, **34**, 437 (2009).
[7] S Bhosle, K Gunasekera, P Boolchand, M Micoulaut. International Journal of Applied Glass Science, **3**, 189 (2012).

[8] H Takebe,H Maeda,K Morinaga. Journal of non-crystalline solids, **291**, 14 (2001).
[9] Y Kawamoto, S Tsuchihashi. Journal of the American Ceramic Society, **54**, 131 (1971).

[10] HP Chen, HZ Tao, QD Wu, XJ Zhao. Journal of the American Ceramic society, **96**, 801 (2013).
[11] S. Onari, O. Sugino, M. Kato, T. Arai, Jpn. Journal of Applied Physics. **21**, 418 (1982) .
[12] T. Wagner, S.O. Kasap, Philos. Mag. B **74**, 667 (1996).
[13] D.G. Georgiev, P. Boolchand, M. Micoulaut, Physical Review B, **62**, R9228 (2000).
[14] T. Petkova, P. Petkov, P. Jovari, I. Kaban, W. Hoyer, A. Schops, A. Webbe, B. Beuneu, Journal of non-crystalline solids, **353**, 2045 (2007).
[15] J. S. Lannin, Physical Review B, **15**, 3863 (1977) .
[16] XC Han, GY Sun, Y Liu, HB Yang. Chalcogenide Letters, **9**, 465 (2012).
[17] X Han, H Tao, L Gong, J Han, S Gu, Chalcogenide Letters, **11**, 181 (2014).
[18] X Han, H Tao, L Gong, XY Wang, XJ Zhao, YZ Yue. Journal of Non-Crystalline Solids, **391**, 117 (2014).
[19] T.S. Moss, T.D.F. Hawkins, Infrared Physics, **1**, 111 (1961)
[20] J.I. Pankove, P. Aigrain, Physical Review, **126**, 956 (1962)
[21] J Mitschele. Journal of Chemical Education, **73**, A260 (1996).
[22] RC Fang. Solid State Spectroscopy. Press of University of Science and Technology of China, Hefei (2001)
[23] J. Tauc. Amorphous and liquid semiconductors. Springer Science & Business Media, New York (2012)
[24] D. Vanderbilt, J.D. Joannopoulos. Physical Review B, **23**, 2596 (1981).
[25] S Kozyukhin, R Golovchak, A Kovalskiy, Semiconductors, **45**, 423 (2011)
[26] D.A. Drabold, Physical Review B, **71**, 054206 (2005).
[27] M Durandurdu, D.A. Drabold, Physical Review B, **65**, 104208 (2002)